

# Lecture I: Searching for non-equilibrium universality in ultracold atomic systems

Ann Arbor, August 9, 2010

Joel E. Moore

University of California, Berkeley  
and Lawrence Berkeley National Laboratory

Work done in collaboration with

**Frank Pollmann**, Subroto Mukerjee, Ari Turner (UCB)

Andrew Green (St. Andrews)

Thanks also to

David Huse, Eduardo Fradkin, Andrew Green, Gil Refael



# Outline of lectures

1. Introduction to nonequilibrium many-particle physics
2. A. More connections between quantum information and condensed matter physics.  
B. Importance of topological defects in spinor condensates.
3. “Topological” phases in condensed matter, and how they might be realized with atoms

# What can condensed matter gain from many-atom and many-ion physics?

1. Maybe atomic physicists can build a quantum computer, to solve all our problems.

2. Maybe atomic physicists will build a quantum *emulator*: a system that replicates the “essentials” of a problem we care about:

Hubbard model (high-temperature superconductivity  
“Topological insulators” Frustrated magnets

3. Maybe atomic physicists will find interesting collective physics in regimes that are difficult to study in condensed matter systems.

# One example of #3: coherent dynamics

In condensed matter systems, the time scale to reach thermal equilibrium is frequently either too short for interesting collective physics to be observed, or too long (e.g., glasses).

When interesting nonequilibrium phenomena have been observed in CM, they have usually been *classical*.

In several atomic physics experiments, the system has been observed on a time scale *long enough for interesting changes, but short enough that the dynamics is coherent.*

# A quantum Newton's cradle

Toshiya Kinoshita<sup>1</sup>, Trevor Wenger<sup>1</sup> & David S. Weiss<sup>1</sup>

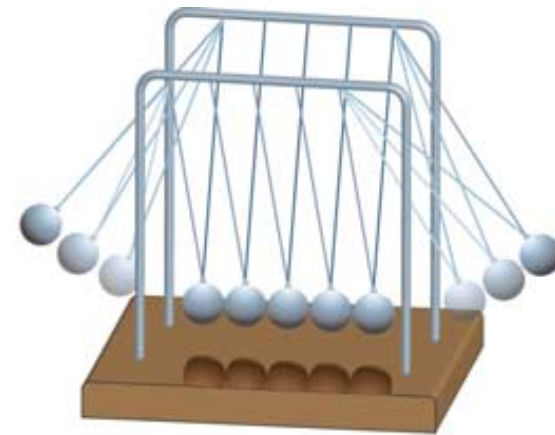
It is a fundamental assumption of statistical mechanics that a closed system with many degrees of freedom ergodically samples all equal energy points in phase space. To understand the limits of this assumption, it is important to find and study systems that are not ergodic, and thus do not reach thermal equilibrium. A few complex systems have been proposed that are expected not to thermalize because their dynamics are integrable<sup>1,2</sup>. Some nearly integrable systems of many particles have been studied numerically, and shown not to ergodically sample phase space<sup>3</sup>. However, there has been no experimental demonstration of such a system with many degrees of freedom that does not approach thermal equilibrium. Here we report the preparation of out-of-equilibrium arrays of trapped one-dimensional (1D) Bose gases, each containing from 40 to 250 <sup>87</sup>Rb atoms, which do not noticeably equilibrate even after thousands of collisions. Our results are probably explainable by the well-known fact that a homogeneous 1D Bose gas with point-like collisional interactions is integrable. Until now, however, the time evolution of out-of-equilibrium 1D Bose gases has been a theoretically unsettled issue<sup>4-6</sup>, as practical factors such as harmonic trapping and imperfectly point-like interactions may compromise integrability. The absence of damping in 1D Bose gases may lead to potential applications in force sensing and atom interferometry.

To see qualitatively why 1D gases might not thermalize, consider the elastic collision of two isolated, identical mass classical particles in one dimension. Energy and momentum are conserved only if they

the prevailing density<sup>14</sup>. The collisions that we study satisfy this criterion well. Our observations extend from the Tonks–Girardeau regime, where only pairwise collisions can occur<sup>15</sup>, to the intermediate coupling regime, where there can be three- (or more) body collisions<sup>15-17</sup>. In both regimes, atoms that are set oscillating and colliding in a trap do not appreciably thermalize during our experiment.

We start our experiments with a Bose–Einstein condensate (BEC) loaded into the combination of a blue-detuned two-dimensional (2D) optical lattice and a red-detuned crossed dipole trap (see Methods). The combination of light traps makes a 2D array of distinct, parallel Bose gases, with the 2D lattice providing tight transverse confinement and the crossed dipole trap providing weak axial trapping<sup>11</sup>. The dynamics within each tube of the 2D array are strictly 1D because the lowest transverse excitation,  $\hbar\omega_r$  (where  $\omega_r/2\pi = 67$  kHz is the transverse oscillation frequency), far exceeds all other energies in

a



## Integrability vs. thermalization in 1D Bose gas

# Integrability vs. thermalization

A classical Hamiltonian system is “integrable” if there are as many independent constants of the motion as there are coordinates.

Such a system is essentially  $N$  harmonic oscillators (with possibly different frequencies). In an infinite-dimensional system, there are extensively many conservation laws, and no thermalization.

The same distinction appears in quantum systems. (The 1D Bose gas with delta-function interactions is “integrable”.)

“Thermalization hypothesis”: evolution, using the Schrödinger equation, of a non-integrable quantum system at *finite energy density* above the ground state leads, after enough time, to

a *pure state* that is locally the same as a *thermal (mixed) state*.

# Spontaneous symmetry breaking in a quenched ferromagnetic spinor Bose-Einstein condensate

L. E. Sadler<sup>1</sup>, J. M. Higbie<sup>1</sup>, S. R. Leslie<sup>1</sup>, M. Vengalattore<sup>1</sup> & D. M. Stamper-Kurn<sup>1</sup>

A central goal in condensed matter and modern atomic physics is the exploration of quantum phases of matter—in particular, how the universal characteristics of zero-temperature quantum phase transitions differ from those established for thermal phase transitions at non-zero temperature. Compared to conventional condensed matter systems, atomic gases provide a unique opportunity to explore quantum dynamics far from equilibrium. For example, gaseous spinor Bose-Einstein condensates<sup>1–3</sup> (whose atoms have non-zero internal angular momentum) are quantum fluids that simultaneously realize superfluidity and magnetism, both of which are associated with symmetry breaking. Here we explore spontaneous symmetry breaking in <sup>87</sup>Rb spinor condensates, rapidly quenched across a quantum phase transition to a ferromagnetic state. We observe the formation of spin textures, ferromagnetic domains and domain walls, and demonstrate phase-sensitive *in situ* detection of spin vortices. The latter are topological defects resulting from the symmetry breaking, containing non-zero spin current but no net mass current<sup>4</sup>.

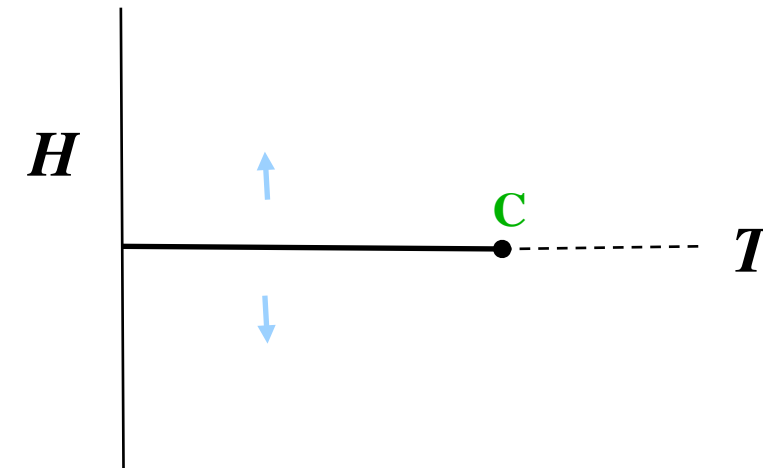
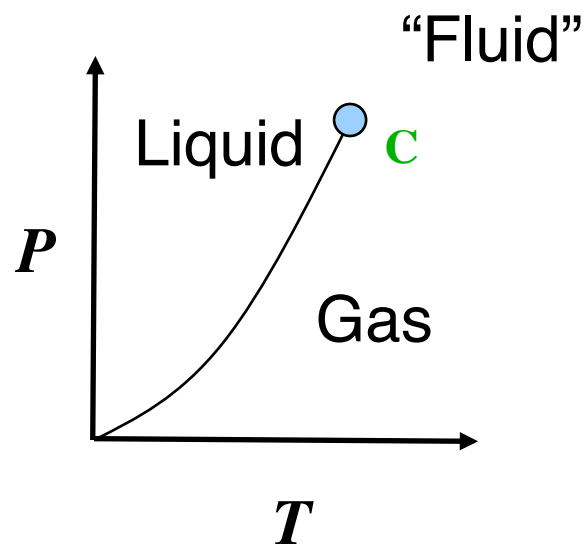
Spinor atomic gases<sup>1–3</sup> are those comprised of atoms with non-

quench, high-resolution maps of the magnetization vector density were obtained using magnetization-sensitive phase-contrast imaging<sup>8</sup>. After the quench, transverse ferromagnetic domains of variable size formed spontaneously throughout the condensate, divided by narrow unmagnetized domain walls. Concurrent with the formation of these domains, we also observed topological defects that we characterize as singly charged spin vortices with circulating spin currents and unmagnetized filled cores.

Spinor BECs in the  $|F = 1, m_z = 0\rangle$  hyperfine state were confined in an optical dipole trap characterized by oscillation frequencies  $(\omega_x, \omega_y, \omega_z) = 2\pi(56, 350, 4.3) \text{ s}^{-1}$ . The condensates, typically containing  $2.1(1) \times 10^6$  atoms, were formed at a magnetic field of 2 G and characterized by a peak density  $n_0 = 2.8 \times 10^{14} \text{ cm}^{-3}$  and Thomas-Fermi radii  $(r_x, r_y, r_z) = (12.8, 2.0, 167) \mu\text{m}$  (see Methods). Variations in the internal-state wavefunction were constrained in these anisotropic condensates to just two spatial dimensions ( $\hat{x}$  and  $\hat{z}$ ) because the spin healing length,  $\xi_s = \sqrt{\hbar^2/2m|c_2|n_0} = 2.4 \mu\text{m}$ , was larger than the cloud size  $r_y$  in the  $\hat{y}$  direction. Thus, imaging the condensate in the  $\hat{x}$ – $\hat{z}$  plane produced complete maps of the magnetization

## Phase-ordering kinetics after quenching across a quantum phase transition

## Basic idea of “universality” at continuous classical phase transitions



Ising (uniaxial) ferromagnet

$$\rho_L - \rho_G \sim \left( \frac{T_C - T}{T_C} \right)^\beta$$

$$M_\uparrow - M_\downarrow \sim \left( \frac{T_C - T}{T_C} \right)^\beta$$

These exponents come from a *classical* theory!

Similar universality appears at continuous quantum ( $T=0$ ) phase transitions and for dynamical quantities:  
we can hope for universal scaling phenomena that are independent of microscopic details.

# Entanglement of single-atom quantum bits at a distance

D. L. Moehring<sup>1</sup>, P. Maunz<sup>1</sup>, S. Olmschenk<sup>1</sup>, K. C. Younge<sup>1</sup>, D. N. Matsukevich<sup>1</sup>, L.-M. Duan<sup>1</sup> & C. Monroe<sup>1,2</sup>

Quantum information science involves the storage, manipulation and communication of information encoded in quantum systems, where the phenomena of superposition and entanglement can provide enhancements over what is possible classically<sup>1,2</sup>. Large-scale quantum information processors require stable and addressable quantum memories, usually in the form of fixed quantum bits (qubits), and a means of transferring and entangling the quantum information between memories that may be separated by macroscopic or even geographic distances. Atomic systems are excellent quantum memories, because appropriate internal electronic states can coherently store qubits over very long timescales. Photons, on the other hand, are the natural platform for the distribution of quantum information between remote qubits, given

separated by one metre. Two remotely located trapped atomic ions each emit a single photon, and the interference and detection of these photons signals the entanglement of the atomic qubits. We characterize the entangled pair by directly measuring qubit correlations with near-perfect detection efficiency. Although this entanglement method is probabilistic, it is still in principle useful for subsequent quantum operations and scalable quantum information applications<sup>18–20</sup>.

In each of two congeneric radio-frequency ion traps, we trap and laser-cool a single  $^{171}\text{Yb}^+$  ion<sup>21</sup>. Each ion is cooled to near the Doppler limit via laser light at 369.5 nm tuned just redward of the  $^2\text{S}_{1/2} \leftrightarrow ^2\text{P}_{1/2}$  atomic resonance. The  $^2\text{P}_{1/2}$  level also has a decay channel to the  $^2\text{D}_{3/2}$  state with a branching ratio of  $\sim 0.005$  (ref. 21). When

## Direct measurement of entanglement, the basic property of quantum information

One connection to previous examples:

*Entanglement* in a quantum coherent system is responsible for the appearance of *entropy* under the “thermalization hypothesis”.

# Quantum entanglement

Sometimes a pure quantum state of a bipartite system  $AB$  is also a pure state of each subsystem separately:

Example:  $S_z=1$  state of two  $s=1/2$  spins,  $A$  and  $B$

$$|\Psi_{AB}\rangle = |\uparrow_A\rangle \otimes |\uparrow_B\rangle$$

a “product” state

Sometimes a pure quantum state of a bipartite system  $AB$  is **not** a pure state of each subsystem separately:

Example: singlet state of two  $s=1/2$  spins

$$|\Psi_{AB}\rangle = \frac{1}{\sqrt{2}} (|\uparrow_A\rangle \otimes |\downarrow_B\rangle - |\downarrow_A\rangle \otimes |\uparrow_B\rangle)$$

an “entangled” state

“Maximal knowledge of the whole does not imply maximal knowledge of the parts”

# Entanglement entropy

$$|\Psi_{AB}\rangle = \frac{1}{\sqrt{2}} (|\uparrow_A\rangle \otimes |\downarrow_B\rangle - |\downarrow_A\rangle \otimes |\uparrow_B\rangle)$$

an “entangled” state

In an entangled state, the state of subsystem A or B is not a pure quantum state, but rather a **density matrix**

For the singlet

$$\rho_A = \begin{pmatrix} \frac{1}{2} & 0 \\ 0 & \frac{1}{2} \end{pmatrix} = \rho_B$$

A classical uncertainty or **entropy** has been created by the operation of looking at only part of the system.

# Entanglement entropy

Definition: the entanglement entropy of a pure state, **with respect to a given partition into A and B**, is the von Neumann entropy of the partial density matrices

$$\langle \phi_1 | \rho_A | \phi_2 \rangle = \sum_j (\langle \phi_1 | \times \langle \psi_j |) | \psi \rangle \langle \psi | (| \phi_2 \rangle \times | \psi_j \rangle)$$

$$S(\rho) = -\text{Tr} \rho_A \log_2 \rho_A = -\text{Tr} \rho_B \log_2 \rho_B$$

In a diagonal basis, this is just  $S = -\sum_i p_i \log_2 p_i$

The singlet generates one bit of classical entropy when the two spins are separated

# Entanglement entropy

Thermalization hypothesis:

for a non-integrable quantum coherent system, the density matrix at long times converges *locally* to that of a thermal system.

$$\langle \phi_1 | \rho_A | \phi_2 \rangle = \sum_j (\langle \phi_1 | \times \langle \psi_j |) | \psi \rangle \langle \psi | (| \phi_2 \rangle \times | \psi_j \rangle)$$

$$S(\rho) = -\text{Tr} \rho_A \log_2 \rho_A = -\text{Tr} \rho_B \log_2 \rho_B$$

Note that the partial density matrix for subsystem A gives the results of *all* experiments limited to A

What we interpret locally as *thermal* entropy must come from *entanglement* entropy if the global system is phase-coherent.

# Spontaneous symmetry breaking in a quenched ferromagnetic spinor Bose-Einstein condensate

L. E. Sadler<sup>1</sup>, J. M. Higbie<sup>1</sup>, S. R. Leslie<sup>1</sup>, M. Vengalattore<sup>1</sup> & D. M. Stamper-Kurn<sup>1</sup>

A central goal in condensed matter and modern atomic physics is the exploration of quantum phases of matter—in particular, how the universal characteristics of zero-temperature quantum phase transitions differ from those established for thermal phase transitions at non-zero temperature. Compared to conventional condensed matter systems, atomic gases provide a unique opportunity to explore quantum dynamics far from equilibrium. For example, gaseous spinor Bose-Einstein condensates<sup>1–3</sup> (whose atoms have non-zero internal angular momentum) are quantum fluids that simultaneously realize superfluidity and magnetism, both of which are associated with symmetry breaking. Here we explore spontaneous symmetry breaking in <sup>87</sup>Rb spinor condensates, rapidly quenched across a quantum phase transition to a ferromagnetic state. We observe the formation of spin textures, ferromagnetic domains and domain walls, and demonstrate phase-sensitive *in situ* detection of spin vortices. The latter are topological defects resulting from the symmetry breaking, containing non-zero spin current but no net mass current<sup>4</sup>.

Spinor atomic gases<sup>1–3</sup> are those comprised of atoms with non-

quench, high-resolution maps of the magnetization vector density were obtained using magnetization-sensitive phase-contrast imaging<sup>8</sup>. After the quench, transverse ferromagnetic domains of variable size formed spontaneously throughout the condensate, divided by narrow unmagnetized domain walls. Concurrent with the formation of these domains, we also observed topological defects that we characterize as singly charged spin vortices with circulating spin currents and unmagnetized filled cores.

Spinor BECs in the  $|F = 1, m_z = 0\rangle$  hyperfine state were confined in an optical dipole trap characterized by oscillation frequencies  $(\omega_x, \omega_y, \omega_z) = 2\pi(56, 350, 4.3) \text{ s}^{-1}$ . The condensates, typically containing  $2.1(1) \times 10^6$  atoms, were formed at a magnetic field of 2 G and characterized by a peak density  $n_0 = 2.8 \times 10^{14} \text{ cm}^{-3}$  and Thomas-Fermi radii  $(r_x, r_y, r_z) = (12.8, 2.0, 167) \mu\text{m}$  (see Methods). Variations in the internal-state wavefunction were constrained in these anisotropic condensates to just two spatial dimensions ( $\hat{x}$  and  $\hat{z}$ ) because the spin healing length,  $\xi_s = \sqrt{\hbar^2/2m|c_2|n_0} = 2.4 \mu\text{m}$ , was larger than the cloud size  $r_y$  in the  $\hat{y}$  direction. Thus, imaging the condensate in the  $\hat{x}$ – $\hat{z}$  plane produced complete maps of the magnetization

First example: spin-1 spinor BEC  
Second example: quantum Ising model  
w/nonintegrable perturbations

# Spin-1 condensate with dipole interaction

(J. Kjall, A. Essin, and J. Moore, 2008)

$$H = \int d^3x \left( \Psi_{\vec{x}}^\dagger \left( -\frac{\nabla^2}{2m} - \mu + B_0 \vec{B} * \vec{F} + q(\vec{B} * \vec{F})^2 \right) \Psi_{\vec{x}} + \frac{c_0}{2} \Psi_{\vec{x}}^\dagger \Psi_{\vec{x}} \Psi_{\vec{x}}^\dagger \Psi_{\vec{x}} + \frac{c_2}{2} \Psi_{\vec{x}}^\dagger \vec{F} \Psi_{\vec{x}} * \Psi_{\vec{x}}^\dagger \vec{F} \Psi_{\vec{x}} \right) + \int d^3x d^3x' \frac{c_d}{2} \Psi_{\vec{x}}^\dagger \vec{F}_i \Psi_{\vec{x}} * \Psi_{\vec{x}'}^\dagger \vec{F}_j \Psi_{\vec{x}'} \nabla_i \nabla_j' \frac{1}{|\vec{r} - \vec{r}'|}$$

Confinement to a two dimensional geometry  $\sigma_n = 4\mu\text{m}$

Typical experimental values  $n_{3D} = 2.2 * 10^{14} \text{ cm}^{-3}$ ,  $B = 150 \text{ mG}$

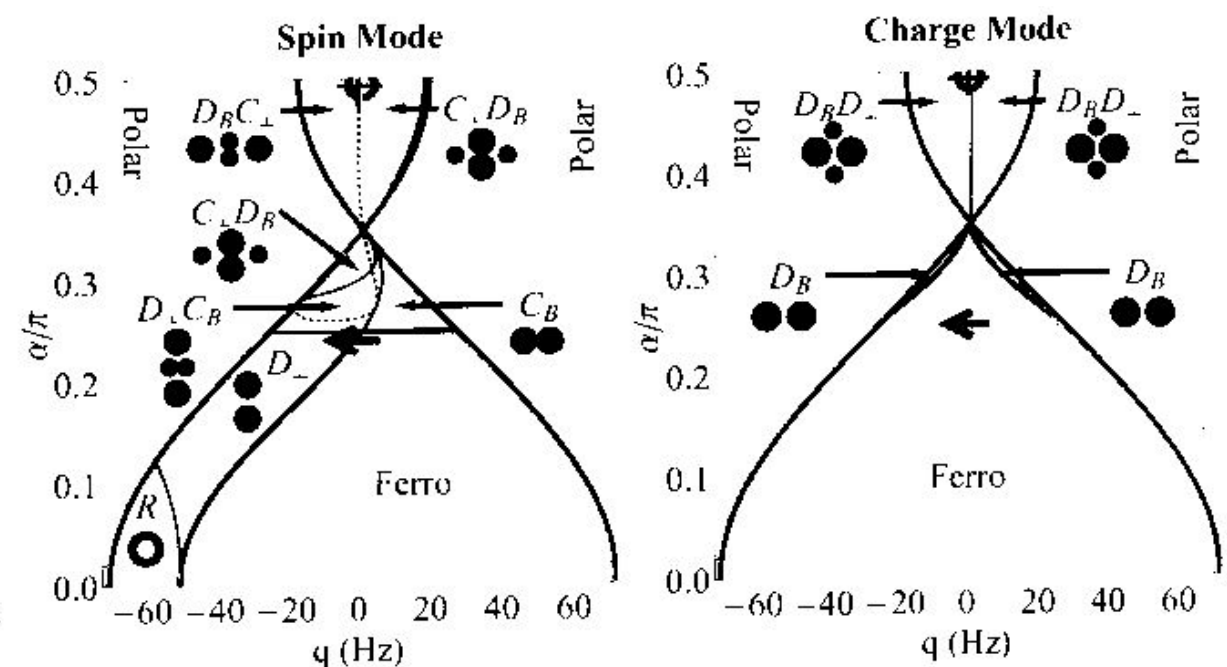
$^{87}\text{Rb}$ :  $c_0 n_{3D} = 1.7 \text{ kHz}$ ,  $c_2 n_{3D} = -8 \text{ Hz}$ ,  $c_d n_{3D} = 10 \text{ Hz}$ ,  $q = 70 \text{ Hz G}^{-2} \text{ B}^2$

(Vengalattore, Stamper-Kurn et.al. 2008)

Average over the rapid Larmor procession

No out of plane dynamics

Spin and charge instabilities important for all  $q$ , indicating a possible tendency towards stripe and checkerboard phases. **Can these be stable?**



(Instability onset diagram, Cherng and Demler arxiv 2008)

# Is the *equilibrium* phase diagram like the instability diagram?

Quadratic Zeeman favors polar state

$c_2 < 0$  favors ferromagnetic state in Rb

Dipole without quadratic Zeeman gives a ferromagnetic state along B

With smaller  $c_0$ , i.e. all energies at the same magnitude, striped/helical phases appear.

No clear checkerboard with the experimental values (at current size); if there is a stable checkerboard, it occupies a small part of the *static* phase diagram.

Upper graph:  $a=30 \mu\text{m}$ ,  $\sigma_n=3 \mu\text{m}$ ,

$c_0 n_{3D}=40 \text{ Hz}$ ,  $c_2 n_{3D}=-8 \text{ Hz}$ ,

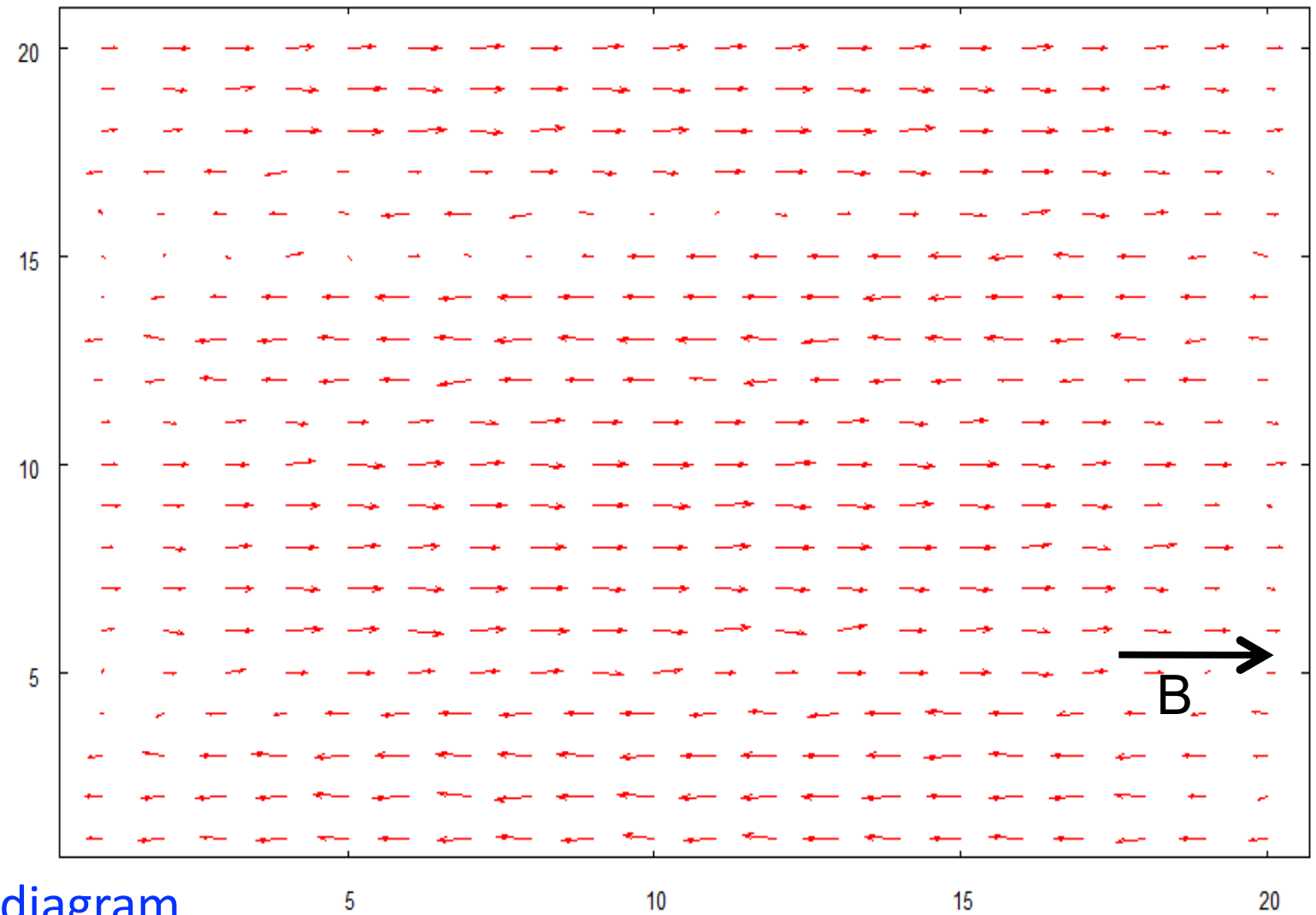
$c_d n_{3D}=10 \text{ Hz}$ ,  $q n_{3D}=-2.5 \text{ Hz}$

Lower graph: transition to polar state, spins along y < 60% ferro.

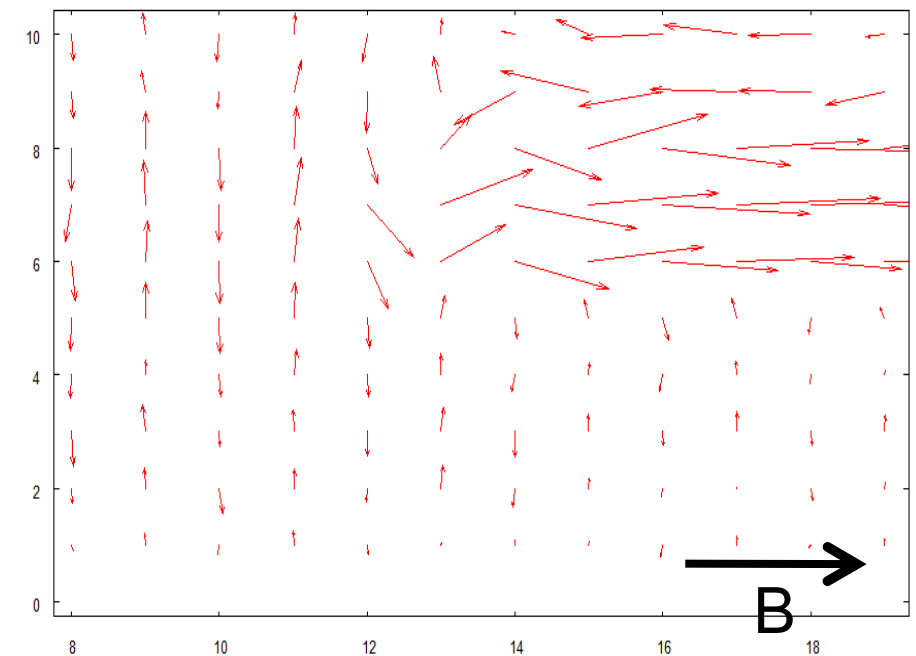
$a=19 \mu\text{m}$ ,  $\sigma_n=3.8 \mu\text{m}$ ,

$c_0 n_{3D}=10 \text{ Hz}$ ,  $c_2 n_{3D}=-8 \text{ Hz}$ ,

$c_d n_{3D}=5 \text{ Hz}$ ,  $q n_{3D}=1.5 \text{ Hz}$



mag. x4



This experiment indicates that **dipole interactions**, and possibly **trap geometry**, can complicate both the phase diagram and dynamics: it seems that the experiment may not reach thermal equilibrium.

In the experiment, the Hamiltonian can be rapidly changed across a phase boundary (a “quantum quench”) to see how a new order is established.

The standard way to study such “phase-ordering kinetics” in condensed matter is by TDGL, a time-dependent version of Ginzburg-Landau theory.

This is still classical dynamics of the order parameter, but an interesting prediction of TDGL is that two models may be in the same **static** universality class but have different **dynamical** universality classes, e.g., different growth of correlation length after a quench.

“Model F” for a spinor condensate:  
second sound density plus condensate dynamics

$$\frac{\partial \psi}{\partial t} = -\Gamma_0 \frac{\delta F_{SS}}{\delta \psi_a^*} - ig_0 \psi \frac{\delta F_{SS}}{\delta m} + \zeta_a(\mathbf{r}, t)$$

$$\frac{\partial m}{\partial t} = \lambda_0^m \nabla^2 \frac{\delta F_{SS}}{\delta m} + 2g_0 \text{Im} \left( \psi_a^* \frac{\delta F_{SS}}{\delta \psi_a^*} \right) + \theta(\mathbf{r}, t)$$

**Remark:** How could the same free energy function give rise to different dynamics?

Think about an electric dipole in an electrical field versus a magnetic dipole in a magnetic field.

Both have the same energy ( $\mu \cdot B$ ), but the magnetic dipole precesses while the electrical dipole oscillates.

The key difference is the commutator/Poisson bracket of various operators with  $H$ .

**But even if a certain TDGL model is correct for the longest time scales at any nonzero temperature, we expect other behavior for intermediate times.**

Two ways to understand this statement:

1. the description in terms of an order parameter plus possibly a few other fields cannot describe the enormous number of possible initial states, including “initial noise” effects; (cf. Lamacraft for spinor BEC)
2. The loss of all phase coherence except in the order parameter field requires that some source of decoherence have acted on all other quantities.

At quantum criticality, for some quantum critical points, we understand the “complexity” of the quantum critical state as reflected e.g. in numerical approaches. (Lecture II)

There are several uses of this idea. Here, we focus on

**Application:** Coherent dynamics near quantum critical points

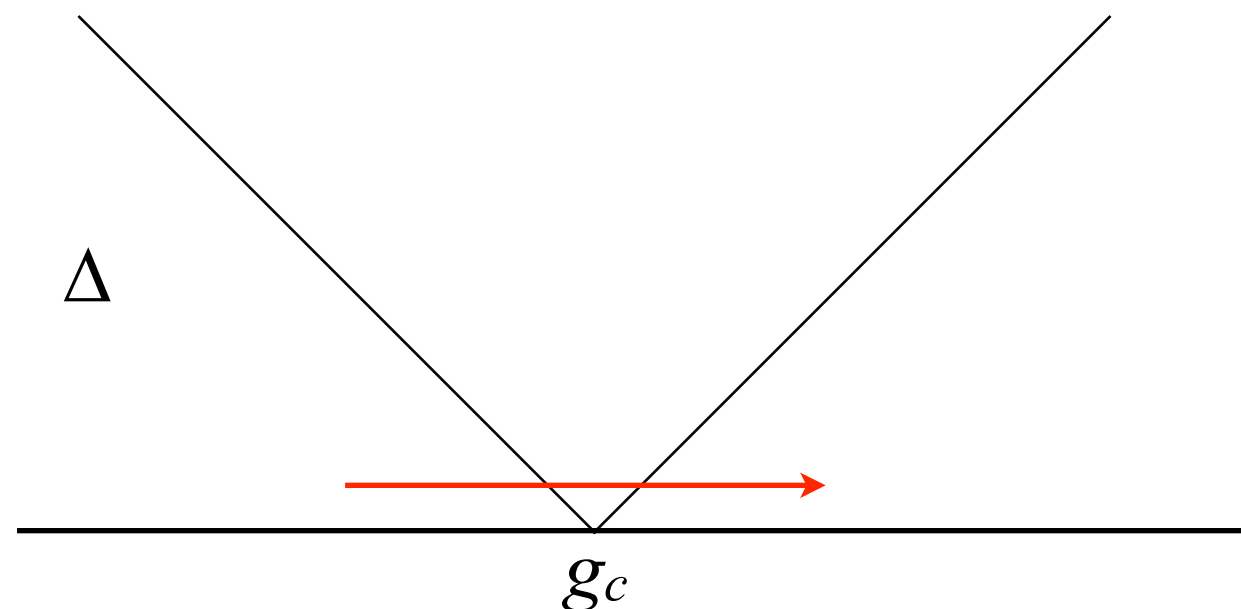
using theoretical ideas that will be explained in the next lecture

## Example 2: Dynamics near quantum critical points

Our motivation:

- We want to control how far a system is excited out of the instantaneous ground state of  $H(t)$ .

We sweep the Hamiltonian slowly through a 1D quantum critical point separating two gapped phases.



$$\begin{aligned}g(t) &= g_i + \Gamma t \\g(0) &= g_i < g_c \\g(t_f) &= g_i + \Gamma t_f > g_c\end{aligned}$$

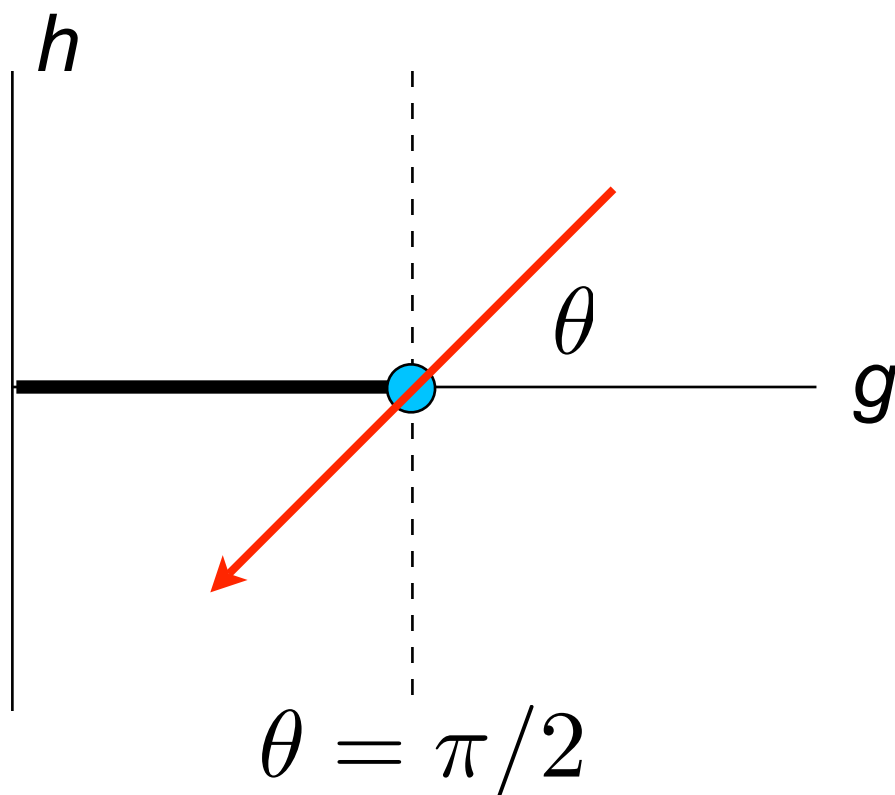
The closing of the gap  $\Delta$  means that deviations from the ground state are power-law in the sweep rate: e.g.,  $E_F - E_0 \sim \Gamma^\alpha$

rather than being exponentially small if  $\Delta > 0$  everywhere (adiabatic theorem).

## Example 2: Dynamics near quantum critical points

- We would like to distinguish integrable and chaotic quantum dynamics, and spontaneous symmetry breaking from explicit symmetry breaking.

Our starting point: cross through the well-studied quantum Ising critical point at various angles in the phase diagram



$$\mathcal{H} = \sum_i \left( \sigma_i^z \sigma_{i+1}^z + g \sigma_{ix} + h \sigma_i^z \right)$$

$$\sin \theta = \frac{h}{g - g_c}, \quad g_c = 1$$

(E8 integrable line, Zamolodchikov)

## Case 1: quantum Ising sweep

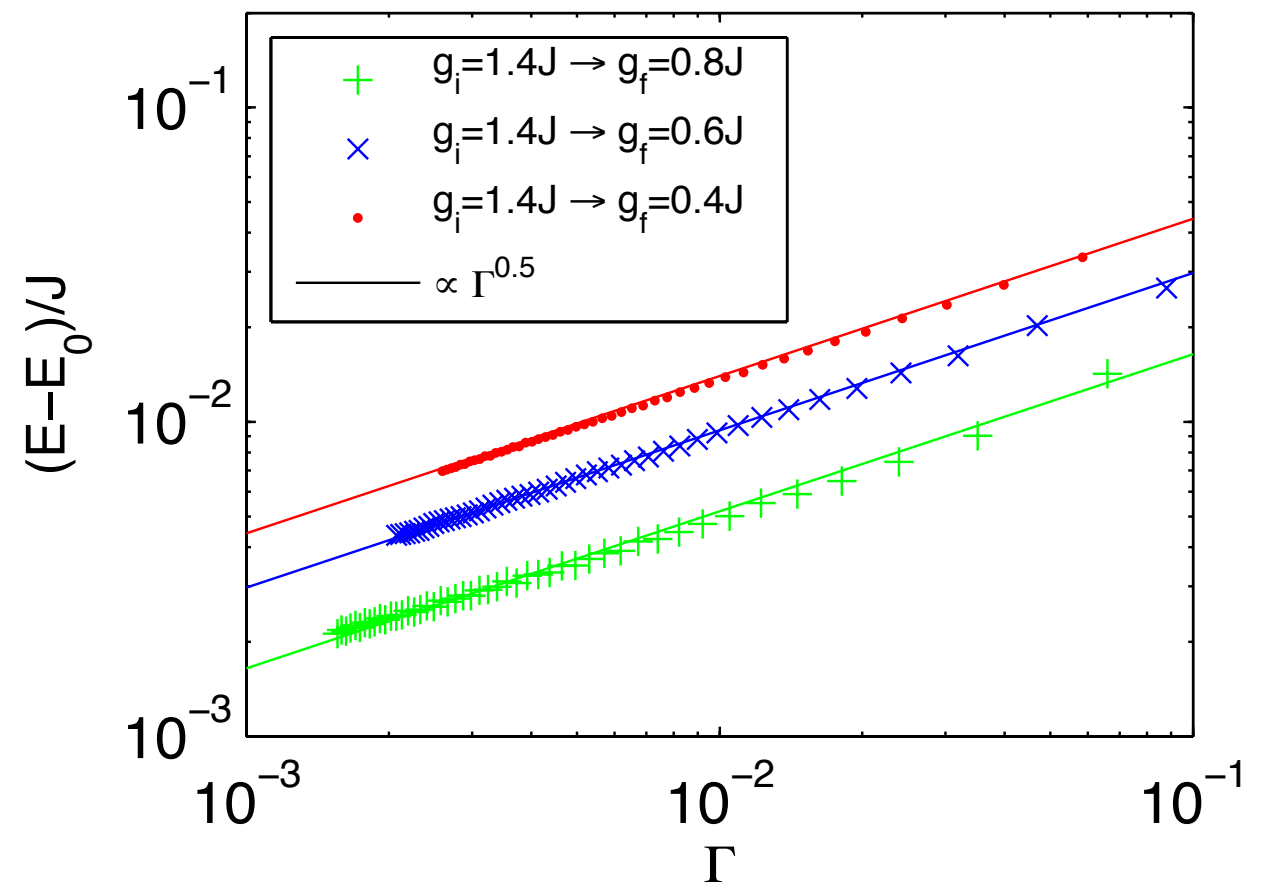
We sweep  $g$  through the critical point at a constant rate.

How different is the resulting state from the ground state?

The energy difference and “number of excitations” are predicted to be related to the sweep rate by a simple scaling law

(Dziarmaga, Polkovnikov, ..)

$$E'_0[g(t)] - E_0[g(t)] \sim n_{\text{ex}} \Delta[g(t)] \sim \Gamma^{d\nu/(z\nu+1)} \Delta[g(t)],$$



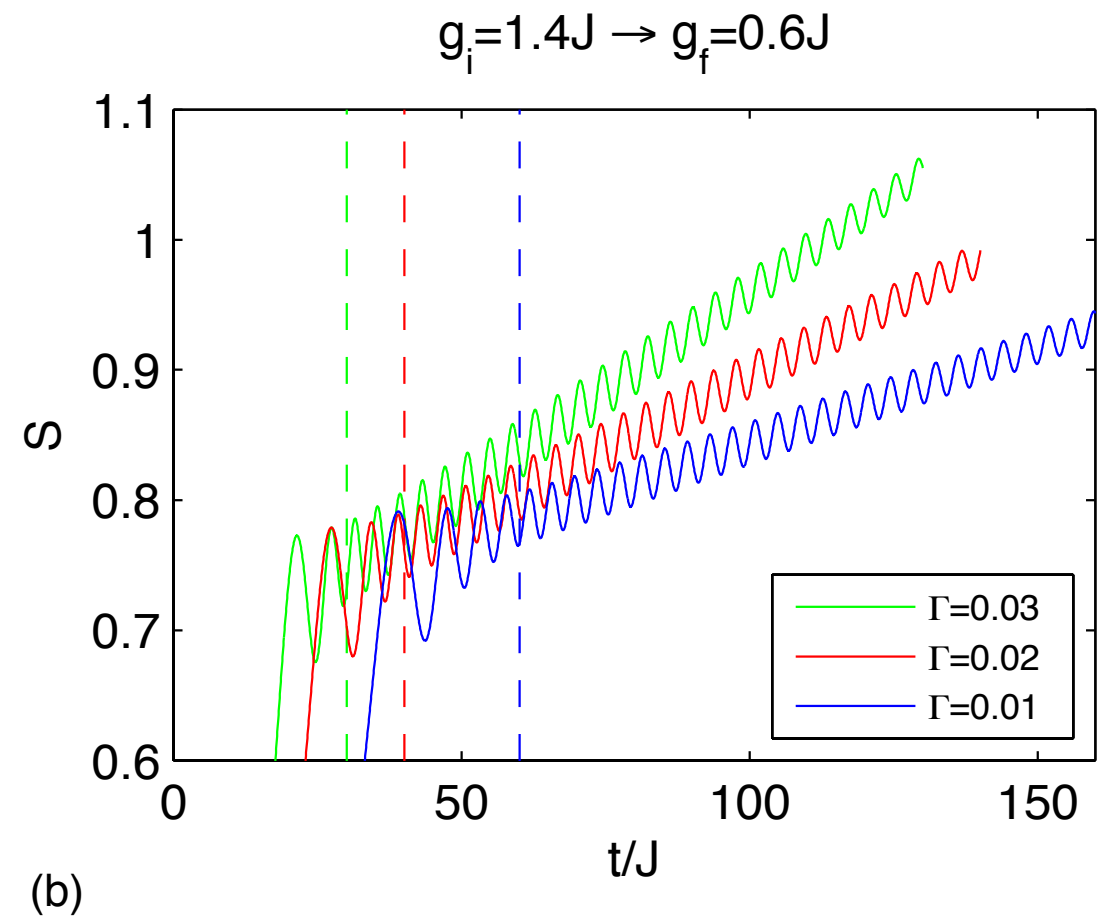
# Case 1: quantum Ising sweep

## Entanglement evolution

We sweep  $g$  through the critical point at a constant rate, then pause at a fixed final value  $g_f$  to observe evolution.

The quantum Ising model has well-defined linearly propagating excitations (“domain walls”). The propagation of these excitations leads to linearly increasing entanglement, even after the sweep has stopped. (cf. Calabrese and Cardy)

This “light-cone” effect depends on the number of excitations created, and hence on the sweep rate.



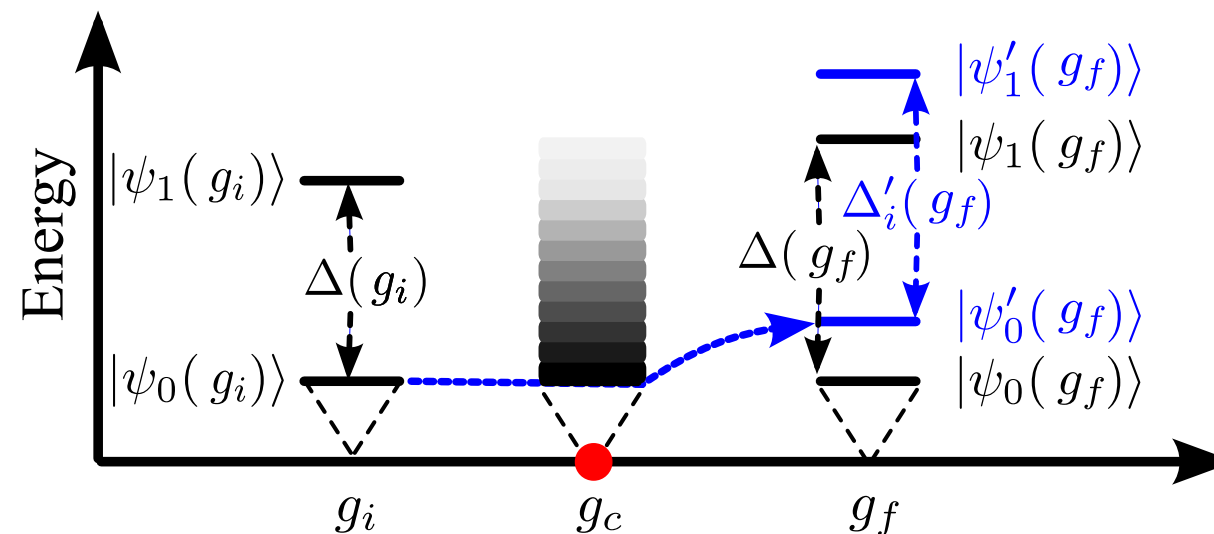
What causes these entanglement oscillations?

## Case 1: quantum Ising sweep

We sweep  $g$  through the critical point at a constant rate, then pause at a fixed final value  $g_f$  to observe evolution.

The oscillations result because, after a slow sweep, the final state consists of a ground state plus excitations at multiples of the final gap.

The small dispersion in final energy leads to a slow decay of the oscillations.



## Application 2: Dynamics near quantum critical points

- Sometimes we want to study quantities that are well-defined in the infinite system, and independent of a particular observable.

We compare states using the spatial decay rate of the “Loschmidt echo” overlap ( $N = \#$  of sites)

$$|\langle \psi_0 | \psi_1 \rangle|^2 \sim \exp(-\alpha N).$$

which is easily computed from the matrix product state representation, and can be found exactly for the quantum Ising case.

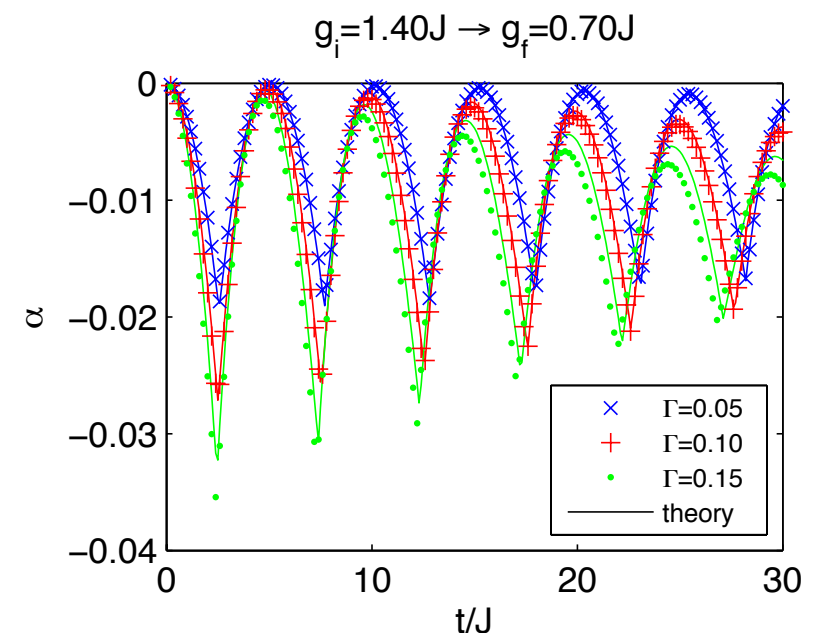
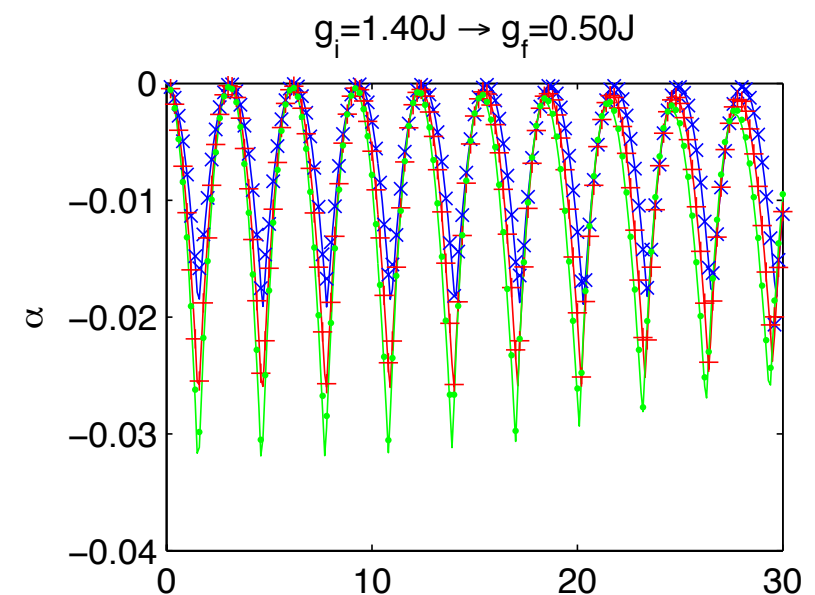
## Case 1: quantum Ising sweep

We sweep  $g$  through the critical point at a constant rate, then pause at a fixed final value  $g_f$  to observe evolution.

We can use the overlap integral to focus on the oscillations and check the TEBD method.

Puzzle: why the nonanalytic dips at certain points in time?

For the quantum Ising model, can compute these exactly using a picture of Landau-Zener tunneling at each momentum  $k$  independently (theory curves shown)...



## Integrable versus non-integrable models

The nonanalytic dips result from a special  $k$  value where the tunneling probability is exactly 1/2. Since this model is integrable, the excitations at this  $k$  have sharp energy.

(Quantum Ising model is “solvable” in a Bogoliubov formalism)

$$|\psi(0)\rangle = \prod_k (u_k |0_k\rangle + v_k |1_k\rangle)$$

$$|v_k|^2 = P_k = 1 - |u_k|^2 = \exp\left(-\frac{2\pi J^2 k^2}{\Gamma}\right)$$

$$|\psi(t)\rangle = \prod_k (u_k |0_k\rangle + e^{-i\Delta_f(k)t/\hbar} v_k |1_k\rangle)$$

Leads to universal  $1/t$  “equilibration” (power-law rather than exponential), *in an integrable system*, resulting just from the continuum of excitation frequencies.

$$\alpha(t) = \frac{1}{2\pi} \int_0^\infty dk \log \left[ (1 - P_k)^2 + P_k^2 + P_k(1 - P_k) \cos(\Delta_f(k)t) \right].$$

(Final state has a diagonal density matrix but is not thermal.)

## Integrable versus non-integrable models

We see similar behavior with different exponents along the other integrable line (2D Ising model in a field).

Along other directions, the model is expected to be non-integrable. For a slow sweep, we see:

at short times the system looks like the integrable case;

beyond some time determined by  $\theta$  and the sweep rate, the “excitations” begin to interact strongly and the cusps are washed out.

This leads to an “entanglement catastrophe”, associated with thermalization, that makes the model difficult to study with our method.

Our current priority: understand what is universal in this process

# Conclusions

1. Ultracold atomic systems can show new types of ordered phases (e.g., the spinor BEC). Moreover, they may show quantum coherent dynamics over a long enough time scale for interesting collective physics before decoherence.

(There are also steady-state phase transitions under driving, which I won't have much to say about.)

2. Dynamics near a quantum critical point can show a weak type of “equilibration” (damped oscillations) in an infinite system even for an integrable system.

3. Entanglement growth, numerical accuracy, and physical properties such as oscillations all seem sensitive to non-integrability.

Some results (e.g., the energy scaling formula for sweeping through a quantum critical point; cf. Polkovnikov) are believed to be general to any dimension. Others will require some nontrivial development to reach  $d > 1$ .

## Conclusions and future directions

1. The finite-entanglement scaling at some critical points can be theoretically predicted.
2. Dynamics near a quantum critical point can show a weak type of “equilibration” (damped oscillations) in an infinite system even for an integrable system.
3. First results on non-integrable dynamics of large quantum systems: Entanglement growth, numerical accuracy, and physical properties such as oscillations all are sensitive to non-integrability.

### Current directions:

Conserved quantities don't equilibrate; generic non-conserved quantities equilibrate exponentially; but some “hydrodynamical” quantities are believed to equilibrate as universal power-laws that are highly nontrivial.

Apply our techniques to specific 1D experimental systems.

Use finite-entanglement scaling like finite-size scaling, to extrapolate numerical results to a larger physical system (like the 2D Hubbard model).